IAEA
International Atomic Energy Agency

20th IAEA Fusion Energy Conference
Vilamoura, Portugal, 1-6 November 2004

IAEA-CN-116/TH/1-5

Density Effects on Tokamak Edge Turbulence and Transport with Magnetic X-points

X.Q. Xu 1), R.H. Cohen 1), W.M. Nevins 1), T.D. Rognlien 1), D.D. Ryutov 1), M.V. Umansky 1), L.D. Pearlstein 1), R.H. Bulmer 1), D.A. Russell 2), J.R. Myra 2), D.A. D'Ippolito 2), M. Greenwald 3), P.B. Snyder 4), M.A. Mahdavi 4)

1) Lawrence Livermore National Laboratory, Livermore, CA 94551 USA
2) Lodestar Research Corporation, Boulder, CO 80301 USA
3) MIT Plasma Science & Fusion Center, Cambridge, MA 02139 USA
4) General Atomics, San Diego, CA 92186 USA

Density Effects on Tokamak Edge Turbulence and Transport with Magnetic X-points[1]

X.Q. Xu 1), R.H. Cohen 1), W.M. Nevins 1), T.D. Rognlien 1), D.D. Ryutov 1), M.V. Umansky 1), L.D. Pearlstein 1), R.H. Bulmer 1), D.A. Russell 2), J.R. Myra 2), D.A. D'Ippolito 2), M. Greenwald 3), P.B. Snyder 4), M.A. Mahdavi 4)

1) Lawrence Livermore National Laboratory, Livermore, CA 94551 USA
2) Lodestar Research Corporation, Boulder, CO 80301 USA
3) MIT Plasma Science & Fusion Center, Cambridge, MA 02139 USA
4) General Atomics, San Diego, CA 92186 USA

e-mail contact of main author: xxu@llnl.gov

Abstract. Results are presented from the 3D electromagnetic turbulence code BOUT, the 2D transport code UEDGE, and theoretical analysis of boundary turbulence and transport in a real divertor-plasma geometry and its relationship to the density limit. Key results include: (1) a transition of the boundary turbulence from resistive X-point to resistive-ballooning as a critical plasma density is exceeded; (2) formation of an X-point MARFE in 2D UEDGE transport simulations for increasing outboard radial transport as found by BOUT for increasing density; (3) identification of convective transport by localized plasma "blobs" in the SOL at high density during neutral fueling, and decorrelation of turbulence between the midplane and the divertor leg due to strong X-point magnetic shear; (4) a new divertor-leg instability driven at high plasma beta by a radial tilt of the divertor plate.

1. Introduction

Achieving high energy confinement at high density is important since the fusion power increases with density as $P_{FUS} \propto n_i^2 \langle \sigma v \rangle$, where n_i is the ion density and $\langle \sigma v \rangle$ is the fusion reaction rate. However, the empirical Greenwald scaling shows that the maximum attainable tokamak plasma density (n_G) is proportional to plasma current, which in turn is limited by MHD kink instabilities [1]. While density limits have been observed for several decades, there is no widely accepted first-principles theory available. Though the empirical scaling is expressed in terms of the line-averaged density, the various experiments suggest that it is an edge phenomenon and that the observed density limit is the result of rapid edge cooling [1].

In this paper, we present a series of studies related to density effects on tokamak edge turbulence and related transport with magnetic X-points [2]. The simulations were carried out primarily using the fluid 3D turbulence code BOUT, and the coupled turbulence and transport BOUT-UEDGE codes [4]. BOUT is a 3D non-local electromagnetic fluid turbulence simulation code and has been updated to include a neutral particle source. The plasma transport is self-consistently driven by boundary turbulence, while neutrals are described by a simple analytic model. The plasma profiles can be evolved simultaneously with the turbulence in the presence of a prescribed heat source from the core plasma and the particle source from the neutrals. The coupled code BOUT-UEDGE has been developed to simulate very

[1]This work was performed under the auspices of the U.S. Department of Energy by University of California Lawrence Livermore National Laboratory under contract No. W-7405-Eng-48 at LLNL, grants DE-FG03-97ER54392 at Lodestar Research, under Contract No. DE-FC02-99ER54512 at MIT, and grants DE-FG03-95ER54309 at general Atomics.

slow physics process in the edge region, such as particle recycling. For toroidally symmetric transport with model cross-field diffusion coefficients and no neutrals, BOUT has been benchmarked with the 2D transport code UEDGE. BOUT simulations demonstrate that boundary turbulence undergoes a transition from resistive X-point to resistive-ballooning, and enhanced radial transport is observed as a critical plasma density is exceeded [2]. The results suggest that large radial transport is a key process for rapid edge cooling, which leads to the tokamak density limit.

The possible presence of a strong instability in the divertor legs, totally decoupled from the main scrape-off layer (SOL), is of significant practical importance. For long-enough legs, the transport produced by this instability would reduce the divertor heat load without having any direct impact on the main SOL, and therefore not lead to the degradation of core confinement. We have considered the effect of finite plasma beta on the divertor-leg instability and finds that, at high-enough betas, unstable, spatially evanescent modes along the field lines that do not reach the X-point region. These localized modes exist only in the presence of the radial tilt of the divertor plate.

The paper is organized as follows: The changing character of turbulence for increasing density is described in Sec. 2. Self-consistent turbulence and transport simulations with a neutral source added is presented in Sec. 3, including blob dynamics and correlation analysis. Section 4 describes the long-time BOUT-UEDGE coupling. The divertor-leg instability is analyzed in Sec. 5. The conclusions are given in Sec. 6.

2. Changing turbulence character with increasing density

A series of BOUT simulations has been conducted to investigate the physical processes which limit the density in tokamak plasmas [2]. In this section, the plasma profiles are frozen, while they are evolved in sections 3 and 4. The background magnetic field structure is obtained from an MHD equilibrium code (*e.g.*, EFIT [5]) for a typical discharge. The plasma profiles of density and electron temperature T_e, are analytic fits (modified tanh) to Thomson scattering data. For scaling studies with plasma density, the plasma pressure is held constant. For scaling studies with plasma current, the background magnetic field structure is obtained from the MHD equilibrium code Corsica [6]. Simulations of turbulence in tokamak boundary plasmas show that turbulent fluctuation levels and transport increase with collisionality. At high edge density, perpendicular turbulent transport dominates parallel classical transport, leading to substantially reduced contact with divertor plates and the destruction of the $\mathbf{E}\times\mathbf{B}$ edge shear layer; the region of high transport then extends inside the last closed magnetic flux surface. As the density increases, these simulations show that the resistive X-point mode transitions to the resistive ballooning mode. The corresponding root-mean-squared (rms) radial-poloidal mode structures are shown in Fig. 1a for three different background densities: $\overline{n}_e = 0.28 n_G$, $\overline{n}_e = 0.56 n_G$, and $\overline{n}_e = 1.12 n_G$. Here $\overline{n}_e$ is the line-averaged density in $10^{20} m^{-3}$, $n_G = I_p/\pi a^2$ in $10^{20} m^{-3}$. For the bottom base case which corresponds to a DIII-D L-mode experiment, $I_p = 0.974$MA, $a = 0.59$m and $\overline{n}_e = 0.25 \times 10^{20} m^{-3}$. The typical resistive X-point mode appears at the bottom of the plot as a base case. In this regime, the X-point effects are the most dramatic. The eigenfunction that has a sharp should illustrates that resistivity is dominant near the X-points, allowing the mode to decrease rapidly away from this region. As density increases, moving vertically up from the bottom of the plot, the rms fluctuation levels increase dramatically, and the modes are poloidally peaked around the

outer midplane. For fixed pressure, as density increases, the temperature decreases, and one enters the strong resistive ballooning regime in the top of the plot. In this case, ballooning of the eigenfunction at the outboard midplane reduces the importance of X-point effects, and it becomes a classical resistive MHD mode. These results clearly demonstrate the transition from resistive X-point mode to resistive ballooning mode as the density approaches and exceeds the Greenwald density.

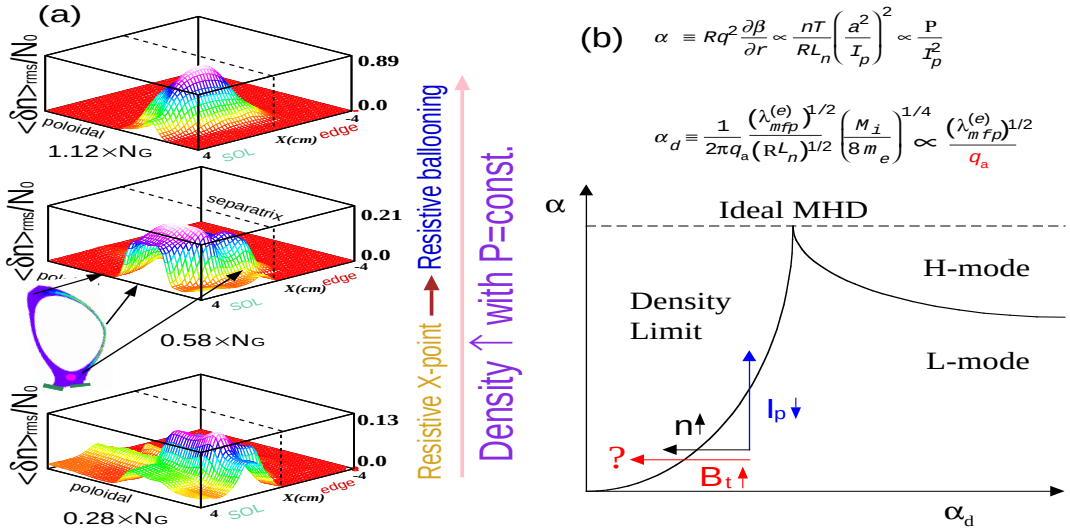

FIG. 1: (a). The rms levels of the radial-poloidal profiles of fluctuation density calculated from BOUT simulation. As the Greenwald density limit is approached or exceeded, the SOL density fluctuation increases and peaks around the outer midplane. Here $N_0 = 1.2 \times 10^{19}/m^3$. *(b). A sketch of edge plasma phase space from Rogers, Drake, and Zeiler theory [7].*

A set of 2D UEDGE transport simulations using increasing outboard convective radial transport to mimic BOUT results for increasing density, shows that this transport can lead to an X-point MARFE when a fixed-fraction carbon impurity radiation is included [2]. This is a common symptom of density-limit related disruptions. BOUT further demonstrates that the current scaling appears on a plot of discharge current versus density as an abrupt increase in radial transport once $\overline{n}_e/n_G > 1$. All of these results indicate that rapid edge cooling due to large radial transport is a key physics element of the tokamak density limit. The simulation results are qualitatively consistent with experimental observations from C-mod and DIII-D [3]. These simulations are qualitatively consistent with previous theory and simulations given by Rogers, Drake, and Zeiler (RDZ) [7], with the exception of the safety factor q-dependence in their α_d scaling. The three sets of simulations are extrapolated to compare with RDZ theory and experiments, and to check whether a density limit boundary line is crossed, as the arrows indicate in Fig. 1b. (1). For fixed q, current I_p and pressure P, an increase in density n_e leads to a fixed α and a decrease in α_d, $\alpha_d \propto \sqrt{\lambda^e_{mfp}} \propto 1/\sqrt{n_e}$. In this case, the density-limit boundary is crossed, and theory, BOUT simulations and experiments agree. (2). For fixed q, temperatures T_e, T_i and density n_e, a decrease in current I_p leads to an increase in $\alpha \approx 1/I_p^2$ and constant α_d. In this case, the density limit boundary is crossed, and theory, BOUT simulations and experiments agree. (3). For fixed I_p, T_e, T_i and n_e, an increase in toroidal magnetic field B_t leads to a fixed α and a decrease in $\alpha_d \approx 1/q$ since $q \propto B_t$. In this case, the RDZ theory predicts a density limit, but both experiments [8] and BOUT find no transition for this case. The disagreement may be due to two important pieces

of physics omitted from RDZ theory that are kept in BOUT simulations: X-point physics and SOL physics. X-point physics limits the mode to the outside midplane such that the parallel connection length qR is not a good measure of the parallel mode width. SOL physics contributes significantly to the formation of the E_r well and our simulations show that the onset of large radial transport is associated with the destruction of the E_r well.

3. Blob dynamics and correlation analysis

For self-consistent turbulence and transport simulations with a neutral source added, we find that as density rises due to neutral fueling, turbulence transport increases. The same trend has been obtained with fixed plasma profiles as discussed in last section. The characteristics of the fluctuations also changed from small scale turbulence to large density structures called blobs. At high density during density ramp-up simulations, we have identified convective transport by localized plasma blobs [9] in the SOL [10]. These properties include: (1) Blob

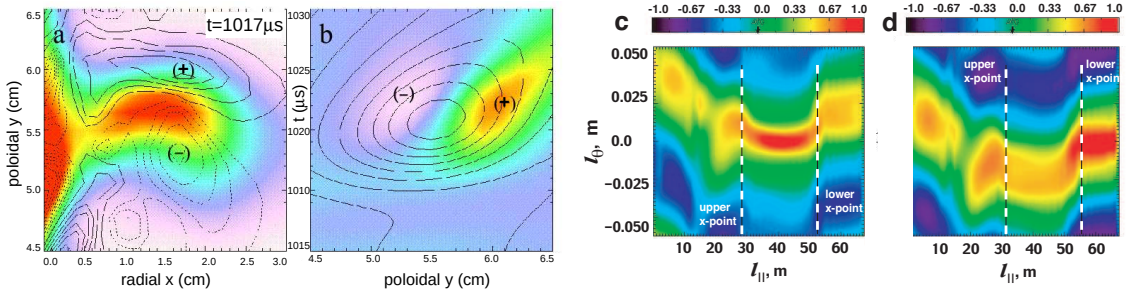

FIG. 2: (a). Blob detached from the separatrix, vorticity over density (color); (b). History of blob vorticity at the wall, density over vorticity (color); (c). Correlation function for reference point at outer midplane vs poloidal and parallel correlation length. (d). Correlation function for reference point at outer divertor leg.

detachment from the separatrix: spatially localized and non-diffusive transport of positive density fluctuations radially outward, as shown in Fig. 2a. (2) Blob translation from dipole vorticity with the $\mathbf{E} \times \mathbf{B}$ drift calculated from potential fluctuations, as shown in Fig. 2b. The self-consistent E-field of the blob is predominantly a dipole field, increasingly as the blob moves away from the separatrix. The radial velocity shows a weak scaling with blob radius, as expected from "disconnected" blob models [10, 11]. (3) Blob rotation (monopole vorticity): observed to decay, probably due to T_e relaxation and/or sheath disconnection. (4) Cross correlation analysis indicates a decorrelation of turbulence between the midplane and the divertor leg due to strong X-point magnetic shear [12]. Figure 2c shows that the cross-correlation has cutoffs near both the lower X-point and the upper X-point regions for reference point at outer midplane, and the cutoff is more pronounced for larger poloidal wavenumber k_θ. Figure 2d shows that the cross-correlation has cutoffs near the X-point regions for reference point at outer divertor leg. It is also shown in Fig. 2c and 2d that the poloidal correlation length is about 1 cm and the parallel correlation length is about 20 meters.

The simulation results also show the density buildup around the separatrix in L-mode during neutral fueling. The simulation data points with different neutral density at the wall and their fit to a "modified tanh fit" formula [13] are plotted in Fig. 3. The main effect of raising the neutral density (aside from raising the overall density) is to increase the density in the far SOL relative to the top of the density profile. The density gradient scale length

parameters are obtained by fitting the modified tanhfit function to the profiles. There is a general overall trend of the formation of "knee" at the base of the profile and the minimum density gradient scale length W_{data} to decrease with increasing density as observed in the experimental data [14]. However, the center position of the modified tanhfit ("knee" at the base of the profile) is moving toward the SOL and the modified tanhfit is no longer the best fit, due to the appearance of large blob structures as the density increases. The flat density profile in the SOL at high neutral density is a feature of convective transport by localized plasma blobs. The detailed blob dynamics for the case of neutral density $N_n = 1 \times 10^{11} cm^{-3}$ in Fig. 3 is shown in Fig. 2a and is analyzed in Ref. [10]. It is also found that the density gradient scale length at the separatrix W_{sep} is roughly constant with increasing density.

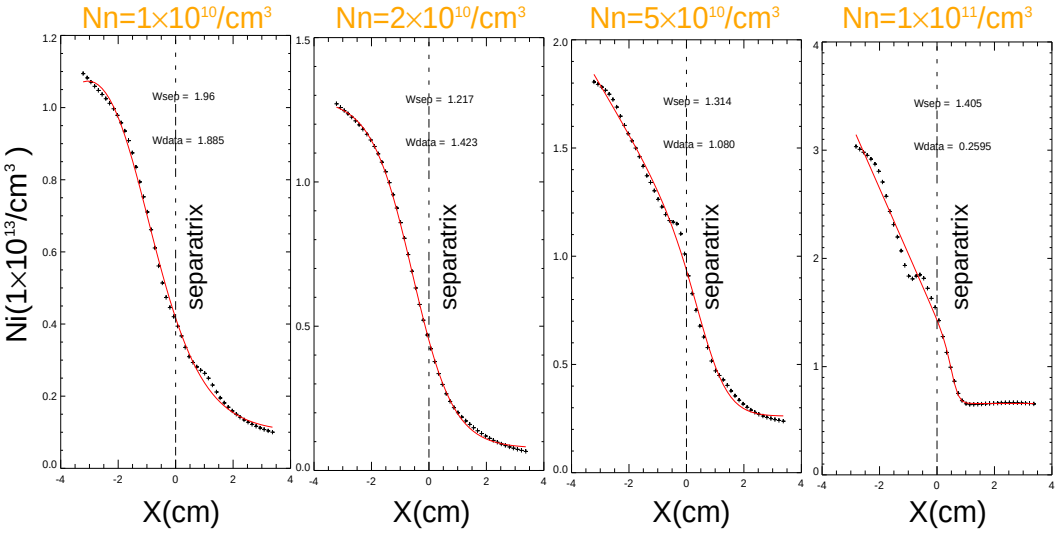

FIG. 3: Background plasma density and its modified tanh fit to the simulation profiles after $\sim 0.5-1 ms$ *evolution vs. neutral density at the outside midplane*

4. Long-time turbulence/profile evolution

As shown above, the turbulence code can evolve profiles over times on the order of 1 ms, which is comparable to the ion transit time from midplane to divertor plate near the separatrix. However, near-unity particle recycling and sputtering from the divertor plates and walls results in edge plasma profile evolution that typically has a time-scale in excess of 10 ms. To treat such long profile evolution, a scheme [18] has be implemented that iteratively couples BOUT turbulence to the 2D axisymmetric UEDGE transport code. For example, the continuity equation for n_i with sources S is separated into two equations, one describing the long-time evolution of the temporally- and toroidally-averaged density, $N_i \equiv \langle n_i \rangle_{\phi,t}$, and the second giving the rapidly varying fluctuations $\tilde{n_i} \equiv n_i - N_i$, yielding

$$\partial_t N_i + \nabla \cdot \langle \Gamma \rangle = \langle S \rangle \quad \text{and} \quad \partial_t \tilde{n_i} + \nabla \cdot (\Gamma - \langle \Gamma \rangle) = S - \langle S \rangle. \tag{1}$$

The radial particle flux, Γ_r, has a large turbulence-induced component provided by the BOUT code in the form $\langle \Gamma_r \rangle = \langle \tilde{n_i} \tilde{v_r} \rangle$, and the turbulence code in turn receives the detailed profile information for N_i from UEDGE that provides a consistent model of neutral sources from divertor and wall recycling. This procedure is efficient compared to straightforward evolution of the full 3D system because a substantial time-scale separation exists in the edge

($\sim$ 0.1 ms for saturation of turbulence and $>$ 10 ms for transport). We focus on a self-consistent statistical steady-state by running each code on its own characteristic time-scale. For numerical stability, a relaxation iteration is used where only a fraction of new plasma fluxes and profile changes are updated on each iteration [18].

The iterative procedure has been used for 4 plasma variables (n_i, $v_{i\|}$, T_e, and T_i) and has produced approximate steady-states after $\sim$ 10 iterations [4]. The neutral recycling model from UEDGE produces plasma profiles in both the radial and poloidal directions (a low T_e, high n_i divertor region). These cases have no E_r well, and thus correspond to the situation where the turbulence has destroyed the well. Both codes have axisymmetric E_r models available, and work is underway to obtain a unified description for H-mode studies.

An example of the turbulence/transport coupling is illustrated in Fig. 4a where the iteration history of the midplane density is shown for a DIII-D single-null configuration with $\sim$2 MW input. The full 2D contour of the effective radial diffusion coefficient after the final 9^{th} iteration is shown in Fig. 4b. Note that the turbulent flux, which has a strong outward convective character in the SOL, can sometimes be represented by a spatially dependent diffusion coefficient as done here. More generally, we use both diffusive and convective terms to match the fluxes. Here the strong ballooning character of the turbulence is very evident.

These cases do show strong plasma fluxes to the main chamber wall, with typically $\sim$30% going to such walls compared to the divertor plates. Nevertheless, owing to the the smaller surface area of the divertor footprint, the density and local H_α intensity there is very much larger than at the walls. Also, these simulations assume a wall conformal to the poloidal magnetic flux surface with a value of 1.1 normalized to the separatrix value; in reality, the wall can be significantly farther away at many toroidal and poloidal positions.

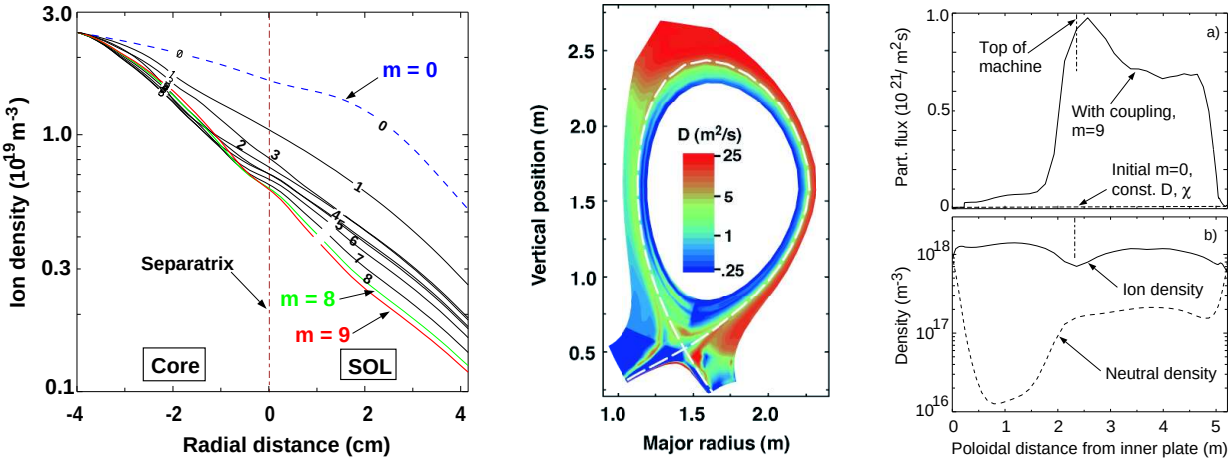

FIG. 4: Left panel: iteration history (m=index) of midplane density for BOUT/UEDGE coupling. Middle panel: effective radial turbulent particle diffusivity after the m=9 iteration. Right panel: particle fluxes to chamber wall after the m=9 iteration with ion and neutral density

5. Finite-beta modes localized near the divertor plate

The simulation data shown in Fig. 2d is suggestive of an instability localized between the divertor plate and the X point, such as that discussed in Ref. [15]. The instability so discussed depended on "boundary conditions" at the X point as well as at the divertor plate. Here we examine the possibility of a mode that is localized near the divertor and does not involve

the X point region at all. We consider the slab geometry shown in Fig. 5a. For simplicity, we assume that the only unperturbed quantity that has spatial variation is the electron temperature, $T_e = T_e(x)$. We consider the case of low recycling, where the plasma flows towards the divertor plate with parallel velocity u exceeding the sound speed.

An unstable mode does not reach the X point if the growth rate is large enough, $\mathrm{Im}\,\Omega > v_A/L$, where L is the characteristic distance from the plate to the X point, and v_A is the Alfven velocity. We make this assumption and determine the limits of validity *a posteriori*. We consider perturbations with $k_x\Delta > 1$, $k_y \gg k_x$, where $\Delta = |T_e/(dT_e/dx)|$. We also assume that $k_y\rho_i \ll 1$, so that one can use a fluid approach (ρ_i is the ion gyroradius) . Then, we impose sheath boundary conditions on the divertor plate, analogous to those described in [16, 17]. This gives rise to the following dispersion relation for evanescent Alfvèn waves:

$$\Omega\left[i\left(v_A + \frac{\omega_{ci}^2 m_i u}{k_y^2 T_e}\right) + \frac{\omega_{ci}}{k}\frac{B_z}{B_y}\tan\alpha\right] = \frac{T_e'}{T_e}\left[i(\Lambda+0.5)\frac{\omega_{ci}u}{k} + \frac{T_e}{m_i}\tan\alpha\right] = 0. \qquad (2)$$

where Λ is the logarithm of the ratio of the electron and ion thermal velocities. In Fig. 5b, we plot the normalized growth rate $\mathrm{Im}\,\tilde{\Omega} = (L/v_A)\,\mathrm{Im}\,\Omega$ vs. the normalized wave-number $\tilde{k} = k_y\rho_i$. We assume that $T_e'\tan\alpha < 0$, i.e., the temperature decreasing in the outward direction, and the plate tilted outward as shown in Fig. 5a. As is clear from Eq. (2), the

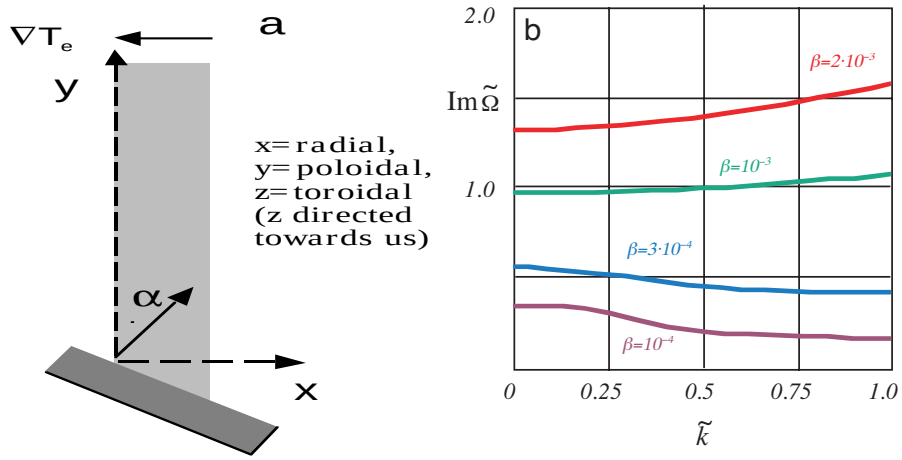

FIG. 5: (a). The geometry of the problem. (b). Normalized growth rate vs normalized wave number for plasma parameters $T_e = T_i = T; u = 2\sqrt{2T/m}; B_z/B_y = 5; \Lambda = 2.5, L/\Delta = 500, \tan\alpha = 10$.

instability is absent in the case of no tilt and increases with increasing outward tilt (or inward tilt in the private-flux region). The physical mechanism is related to the additional force acting on the flux tube displaced along the surface of the tilted plate [15, 16]. Fig. 5b shows that the localized mode exists ($\mathrm{Im}\,\tilde{\Omega} > 1$) only if the plasma beta is high enough. For the parameters chosen for Fig. 5b, β must be higher than 10^{-3}. For smaller β, the instability transitions to that studied in Ref. [15].

6. Summary and conclusions

This paper presents recent analyses of density effects on tokamak turbulence and transport with X-points. These unique comprehensive studies are based on edge turbulence and transport from BOUT and UEDGE simulations, and analytic stability theory. The results are new and significant. We show that as density rises, the fluctuation is changed from resistive

X-point mode to resistive ballooning mode, from small scale turbulence to large blobs. In the large blob regime at high density, the enhanced radial transport as shown can lead to rapid edge cooling, which leads to the density limit. The description given here is consistent with recent experiments on C-Mod [19]. Our theoretical analysis finds a new divertor-leg instability in the finite-beta regime due to a radial tilt of the divertor plate. This instability would produce transport that reduces the divertor heat load while having no direct impact on the upper SOL, which is a desirable ingredient of divertor design. In summary, our results shed light on the qualitative trend and scalings, and provide suggestions of possible experimental control techniques. The successful development of the coupling of the BOUT and UEDGE codes offers a state-of-the-art edge fluid simulation capability, self-consistently including turbulence, transport, and neutrals.

References

[1] GREENWALD, M., TERRY, J.L., *et al.* Nucl. Fusion **28** (1988) 2199; GREENWALD, M., Plasma Phys. Control. Fusion **44**, R27-R80(2002).

[2] XU, X.Q., NEVINS, W.M., *et al.* Phys. Plasmas **10** (2003) 1773.

[3] LABOMBARD,B.,BOIVIN,R.,GREENWALD,M.,*et al.*, Phys. Plasmas **8**, 2107(2001); BEODO, J., RUDAKOV, D. L., MOYER, R., *et al.*, Phys. Plasmas **10**, 1670(2003).

[4] ROGNLIEN, T.D., UMANSKY, M.V., *et al.* Contrib. Plasma Phys. **44** (2004) 188; also J. Nucl. Mater., accepted (2004).

[5] LAO, L.L., ST. JOHN, H,. *et al.* Nucl. Fusion **25** (1985) 1611.

[6] PEARLSTEIN, L.D., *et al.* Proc. 28th EPS Conf. Controlled Fusion Plasma Phys, Madeira, Portugal, June 2001, (EPS, Funchal, 2001), Vol. 25A (ECA), p. 1901;

[7] ROGERS, B.N., DRAKE, J.F., *et al.* Phys. Rev. Lett. **81** (1998) 4396.

[8] PETRIE, T.W., KELLMAN, A.G., *et al.* Nucl. Fusion **33** (1993) 929.

[9] KRASHENINNIKOV, S.I., Phys. Lett. A **283** 368(2001).

[10] RUSSELL, D.A., D'IPPOLITO, D.A., *et al.*, submitted, Phys. Rev. Lett. (2004).

[11] D'IPPOLITO, D.A., MYRA, J.R., RUSSELL, D.A., *et al.*, this conference.

[12] UMANSKY, M.V.,*et al.*, Contr. Plasma Phys. **44**, 182(2004); J. Nucl. Mater., (2004).

[13] XU, X.Q., NEVINS,W.M., *et al.*, Contr. Plasma Phys. **44** (2004) 105.

[14] GROEBNER, R.J., MAHDAVI, M.A., *et al.* 19th IAEA Fusion Energy Conference (Lyon, France, 14 to 19 October 2002), IAEA-CN-94/EX/C2-3.

[15] RYUTOV, D.D, and COHEN, R.H., Contr. Plasma Phys. **44** (2004) 168.

[16] FARINA, D., POZZOLI, R., *et al.*, Plasma Phys. Contr. Fusion, **35**, 1271(1993).

[17] COHEN, R. H., RYUTOV, D. D., Phys. Plasmas, **2**, 2011 (1995).

[18] SHESTAKOV, A.I., COHEN, R.H., *et al.*, J. Comp. Phys. **185**, 399 (2003).

[19] TERRY, J.L., ZWEBEN, S. J., *et al.*, Phys. Plasmas, **10**, 1739 (2003); Jerry, T. L., also this conf.